Assessing the Long-Term Stability of Fatty Acids for Latent Heat Storage by Studying their Thermal Degradation Kinetics

Rocío Bayón[1], Aristides Bonanos[2] and Esther Rojas[1]

[1] CIEMAT-PSA, Madrid (Spain)

[2] The Cyprus Institute, Nicosia (Cyprus)

Abstract

The thermal degradation kinetics of lauric acid has been studied with the aim of assessing its long-term stability and performance as a latent heat storage medium for low temperature applications. For this purpose, dynamic thermogravimetric (TG) measurements were carried out under different gas atmospheres (N_2 and air) and at various heating rates. The kinetic analysis of TG curves assuming a zero-order evaporation process led to activation energy values very close to the evaporation enthalpy although the simulated dα/dT curves could not reproduce the ones experimentally obtained. On the other hand, the analysis of TG measurements with a model-free isoconversional method has shown that the activation energy significantly varies with the degree of conversion. All these results indicate that thermal degradation of lauric acid is a multi-step process whose single-step mechanisms have to be identified. A deconvolution analysis of dα/dT curves was performed by using Fraser-Suzuki functions so that two single-step reaction mechanisms were proposed: the first associated with the evaporation with an activation energy value of 83±8 kJ/mol, while the other may be related to the emission of volatile compounds. The activation energy value of the second mechanism is lower when lauric acid is heated up in air, which may indicate that O_2 is involved in the reaction. The calculated TG curves, assuming the occurrence of these two mechanisms, fit very well to the corresponding experimental curves. Isothermal degradation curves have been calculated by considering both mechanisms and, according to them, lauric acid should totally disappear after 30 days if it is kept under N_2 at 5 ºC above its melting temperature. However preliminary isothermal test in an oven with small samples (in the range of few grams) disagree with those predictions. Hence further isothermal experiments under conditions closer to the real service ones are required in order obtain reliable isothermal degradation curves and assess long-term stability of lauric acid.

Keywords: PCM, lauric acid, TG measurements, kinetic analysis, multi-step processes

1. Introduction

Phase change materials (PCM) with melting temperatures (T_m) between 30 ºC and 70 °C are of particular interest for solar thermal energy storage in the low-temperature range. One of the most critical issues when choosing a PCM for a certain storage application is its long-term performance, which is normally assessed through melting/freezing cycles. However, if a PCM undergoes some kind of degradation after melting due to a chemical reaction or phase segregation, it will be hindered during the freezing period. Hence this kind of tests is not sufficient for validating the successful life-performance of a PCM. Another way to assess long-term stability of PCMs is to carry out kinetic studies of possible degradation processes (Bayón and Rojas, 2019). If a PCM undergoes degradation due to the occurrence of chemical reactions in liquid state, thermogravimetric (TG) measurements can be used for determining the kinetics of such reactions (Vyazovkin et al. 2011). The starting point for the kinetic analysis of TG measurements is the equation which defines the reaction rate:

$$\frac{d\alpha}{dt} = Ae^{\left(\frac{-E}{RT}\right)}f(\alpha) \qquad \text{(eq. 1)}$$

where α is the degree of conversion at a certain time, calculated from TG experimental data and normally expressed in mass loss percentage ($\alpha = 1 - TG(\%)/100$). *A*, *E* and *R* are the frequency factor, the activation energy and the molar gas constant, all present in the Arrhenius law for the reaction rate constant and *f(α)* is a function whose form depends on the mathematical model describing the reaction mechanism. In a dynamic TG

doi:10.18086/eurosun.2020.07.10 Available at http://proceedings.ises.org

measurement performed at constant heating rate $\beta = \frac{dT}{dt}$, (eq. 1) becomes:

$$\frac{d\alpha}{dT} = \frac{Af(\alpha)e^{-E/RT}}{\beta} \quad \text{(eq. 2)}$$

This equation corresponds to the slope of the TG curve in each point, in other words to the dTG (=derivative) curve obtained during the experiments but expressed in terms of α. Therefore, by integrating (eq. 2), the equation of TG curve (α vs. T) can be calculated:

$$\int_0^{\alpha} \frac{d\alpha}{f(\alpha)} = g(\alpha) = \frac{A}{\beta}\int_{T_0}^{T} e^{-E/RT}dT = \frac{AE}{\beta R}p\left(\frac{E}{RT}\right) \quad \text{(eq. 3)}$$

Similarly to *f(α)*, the *g(α)* function depends on the model used to describe the reaction mechanism (Vyazovkin et al. 2011) whereas *p(E/RT)* is the temperature integral (Doyle, 1961). Since this integral cannot be calculated explicitly, either numerical methods or analytical approximations have been proposed by different authors (Órfão, 2007) for its evaluation.

The aim of any kinetic analysis is to obtain the kinetic triplet: *E, A* and *f(α)*. This can be accomplished by applying either model-fitting methods or model-free isoconversional methods (Vyazovkin et al. 2011). If the reaction mechanism is unknown, the activation energy, *E*, can be estimated with any of the most accurate isoconversional methods (Coats and Redfern, 1964; Akahira and Sunose, 1971; Miura and Maki, 1998). Once the activation energy is obtained, the frequency factor, *A*, and the reaction mechanism, *f(α)*, must also be determined. If the process under study obeys single-step kinetics, meaning that *E* does not vary significantly with α, several methods can be used for obtaining both *A* and *f(α)* or *g(α)*: Kissinger method (Kissinger, 1957), Coats-Redfern method with discriminating approach (Coats and Redfern, 1964) or the method of master plots (Vyazovkin et al. 2011) are some examples.

Conversely, for multi-step processes, the *E* calculated with the isoconversional methods is expected to change with α due to the different relative contributions of each single-step to the overall reaction rate. The occurrence of multi-step processes can also be detected if the dTG curve does not present a unique maximum for the reaction rate but is composed of a series of peaks, which may or may not overlap. In this case, each reaction mechanism or step should be somehow separated and analyzed independently. One way to separate overlapping rate peaks is to perform a deconvolution analysis by using mathematical functions that have peak shapes (Vyazovkin et al. 2020). Since the rate peaks of single-step reactions generally exhibit asymmetric shapes, one of the most commonly used function for deconvoluting dTG curves is the Fraser-Suzuki function (Fraser and Suzuki, 1969; Rusch and Lelieur, 1973). Many examples can be found in the literature in relation to the use of Fraser-Suzuki (*FS*) functions in the kinetic analysis of TG measurements of different kinds of materials (Perejón et al., 2011; Cheng et al., 2015; Stankovic et al., 2018). Once the single-step processes have been identified, the kinetic triplet for each reaction mechanism can be obtained by applying any of the above mentioned methods (Kissinger, 1957; Coats and Redfern, 1964; Vyazovkin et al. 2011).

Fatty acids, either pure or their mixtures, are among the PCM whose melting temperature is in the range of 30 ºC to 70 ºC. Some previous studies of various fatty acids have demonstrated that their thermal properties (i.e. melting temperature and enthalpy) do not significantly change after up to 3000 consecutive melting/freezing cycles (Kahwaji, 2017). However, up to now, no degradation studies from the kinetic point of view have been carried out for these PCMs. Hence long-term performance of fatty acids as latent storage materials is still not fully assessed.

Being aware of this problem, in the Thermal Storage Unit of CIEMAT-PSA we aim to study the degradation kinetics of various straight-chain fatty acids normally used as PCM. In this work we present the results obtained up to now for dodecanoic acid ($C_{11}H_{23}$-COOH), also known as lauric acid with a melting temperature of T_m=45 ºC. For this purpose, dynamic thermogravimetric (TG) measurements have been performed with different heating rates under either N_2 or air. The analysis of TG results by a model-free isoconversional method has shown an important variation of the activation energy with conversion, which supports the occurrence of multi-step processes. Hence deconvolution of dTG curves has been performed for separating the single-step reaction processes and obtaining the corresponding Arrhenius parameters together with the possible reaction mechanisms. Finally the TG curves have been simulated and compared with the experimental ones and the isothermal degradation curves have been calculated and discussed.

2. Experimental

The lauric acid used in this work had >98% purity and was supplied by Sigma-Aldrich. Dynamic thermogravimetric (TG) analysis was performed in a TGA Q500 apparatus from TA Instruments®. TG measurements were carried out for samples of 10-12 mg with heating rates, β, ranging from 1 ºC/min to 20 ºC/min under either N_2 or air atmosphere at 90 ml/min. The results of TG analysis are mass-loss percentage curves TG (%) and the corresponding derivative curves dTG (%/K) expressed as a function of temperature one for each heating rate, β. Examples of both sets of curves are displayed in Fig. 1 for the case of lauric acid measured under N_2 atmosphere.

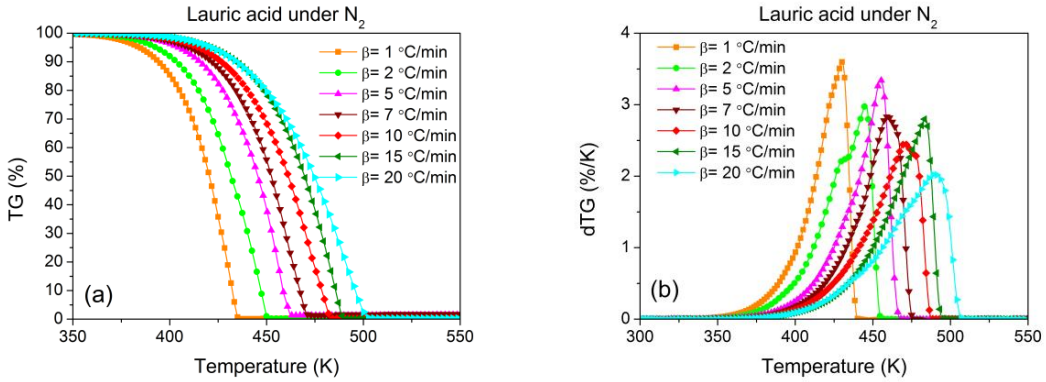

Fig. 1. Experimental TG (%) (a) and dTG (%/K) (b) curves obtained for lauric acid under N_2.

3. Results and discussion

3.1. Estimation of the activation energy, *E*

In principle, straight-chain fatty acids are expected to undergo evaporation upon heating. According to the literature (Penner, 1952), evaporation can be considered as a zero-order mechanism (F0) for which $f(\alpha)=1$, so that (eq. 2) expressed in logarithmic form becomes:

$$\ln\frac{d\alpha}{dT} = \ln\frac{A}{\beta} - \frac{E}{RT} \qquad \text{(eq. 4)}$$

By this linear plot, both the activation energy and the pre-exponential factor can be calculated directly from dTG curve expressed in terms of α. Shen and Alexander already studied the evaporation kinetics of various fatty acids by applying (eq. 4) to dTG curves measured under N_2 (100 ml/min) at 2 ºC/min (Shen and Alexander, 1999). They took the curve at the lowest heating rate because in suchcases the system is expected to be closer to the thermodynamic equilibrium (Arias et al., 2009). In order to compare with their results, we also applied this method to our dTG curves measured at 2 ºC/min under both N_2 and air (90 ml/min) atmospheres. The *E* and *logA* values reported by Shen and Alexander are recorded in Table 1 together with the corresponding values obtained in this work. For the activation energy, our values are slightly higher than the obtained by these authors but in any case, they are still quite close to the evaporation enthalpy calculated from Clausius-Clapeyron and Antoine equations (ΔH_{evap}=82.92 kJ/mol) (Shen and Alexander, 1999). This supports the fact that evaporation of lauric acid is occurring. As for the *logA*, our values seem to be slightly lower than the one reported by Shen and Alexander if min^{-1} units are assumed for *A*. However, the results cannot be compared since these authors do not give information about the corresponding units of *A*.

Table 1. Arrhenius parameters (E and logA) obtained by Shen and Alexander, 1999 and in this work by assuming a zero-order evaporation process for lauric acid under N_2 and air.

Ref.	*Atmosphere*	*E (kJ/mol)*	*logA*
Shen and Alexander, 1999	N_2	81.98	9.72 (-)
This work	N_2	83.10	8.96 (min^{-1}) or 7.18 (s^{-1})
This work	air	83.80	9.08 (min^{-1}) or 7.30 (s^{-1})

By using this method we also calculated the Arrhenius parameters for the dTG curve measured under both N_2 and air at β=1 ºC/min, the lowest heating rate in our set of experiments. In Fig. 2 (a) and (b) the corresponding linear plots of (eq. 4) are displayed for such rate together with the values of E and $logA$ (min^{-1}) obtained. As we can see, the linear fitting is very good for the curves measured under both atmospheres.

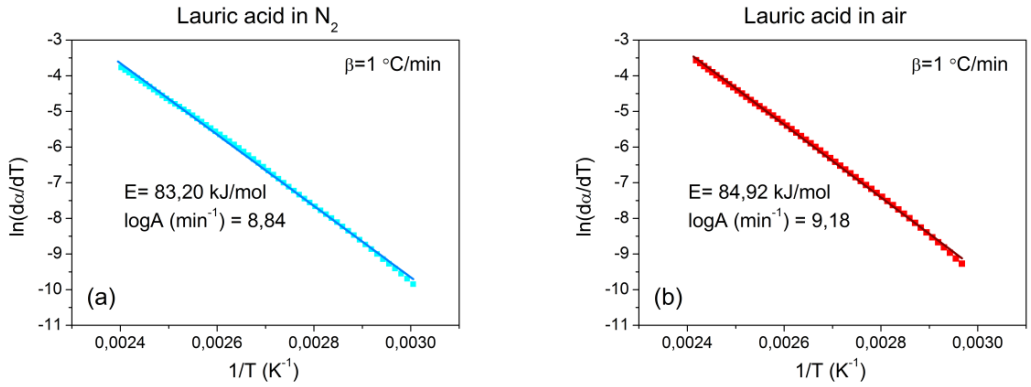

Fig. 2. Linear plot of (eq. 4) for dTG curve of lauric acid at β=1ºC/min under both N_2 (a) and air (b).

The dTG curves have been simulated with (eq. 2) by assuming a zero-order mechanism ($f(\alpha)$=1) and taking the Arrhenius parameters obtained for β=1 ºC/min. In Fig. 3 the resulting dTG curves have been compared with the experimental ones for lauric acid under N_2 at β=1 ºC/min and β=20 ºC/min (a) and under air at β=1 ºC/min and β=15 ºC/min (b). For both atmospheres we can see that the simulated dTG curves for low heating rates fit quite well the experimental data. However, for high heating rates, the simulated curves do not represent the thermal behavior of lauric acid. Hence, this indicates that in addition to vaporization, other degradation mechanisms are taking place when lauric acid is heated.

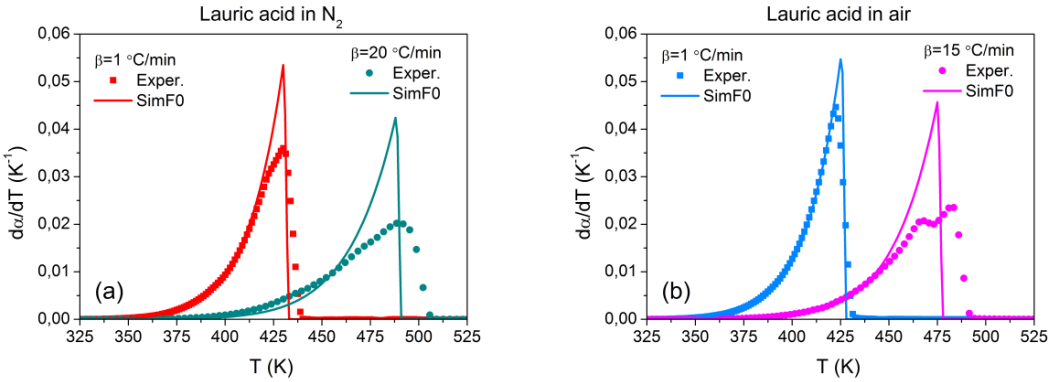

Fig. 3 Simulation of dTG curves for f(α)=1 and the Arrhenius parameters of Fig. 2 and comparison with the experimental data of lauric acid under N_2 at β= 1ºC/min and β= 20 ºC/min (a) and under air at β= 1ºC/min and β= 15 ºC/min (b).

In order to improve the kinetic analysis of TG measurements, a model-free isoconversional method was applied. This kind of methods allows estimating the activation energy as a function of α without choosing any model, $f(\alpha)$, for the reaction mechanism. The basic assumption of these methods is that the reaction rate at constant extent of conversion, α, depends only on temperature, so that constant E values can be expected. Some of the most accurate isoconversional methods (Coats and Redfern, 1964; Akahira and Sunose, 1971; Miura and Maki, 1998) are based on linear expressions like:

$$\ln\frac{\beta}{T^2} = Constant\ -\frac{E}{RT} \qquad \text{(eq. 5)}$$

From a set of TG curves obtained at different heating rates and taking the temperatures at which a certain degree of conversion occurs, the activation energy can be obtained from the slope of the linear plot of (eq. 5). Fig. 4 (a) shows $\ln(\beta/T^2)\ vs.\ 1/T$ plot and the corresponding linear fit for TG measurements of lauric acid under N_2 and air at α=0.5. By using the same procedure, the activation energy was calculated for other conversion values and the results are displayed in Fig. 4 (b) together with the E values obtained from the linear fits of Fig. 2. We can

clearly see that *E* varies significantly with α not only for the case of lauric acid under N_2 but also for the case of air atmosphere. On the other hand, comparing with the *E* values obtained from the plot of (eq. 4) (see Fig. 2), strong differences are observed. For the case of lauric acid under N_2, as we move towards high conversion degrees, *E* values approach a constant value very close to the one obtained with (eq. 4) and hence to the evaporation enthalpy. Similar behavior was observed by other authors for caprylic acid (Arias et al., 2009). However, for the case of lauric acid under air, the variation of *E* with α not only does not approach a constant value but decreases almost linearly as conversion increases. Moreover, in Fig. 4 we can see that *E* is well below the value obtained from the plot of (eq. 4) for the case of lauric acid under air.

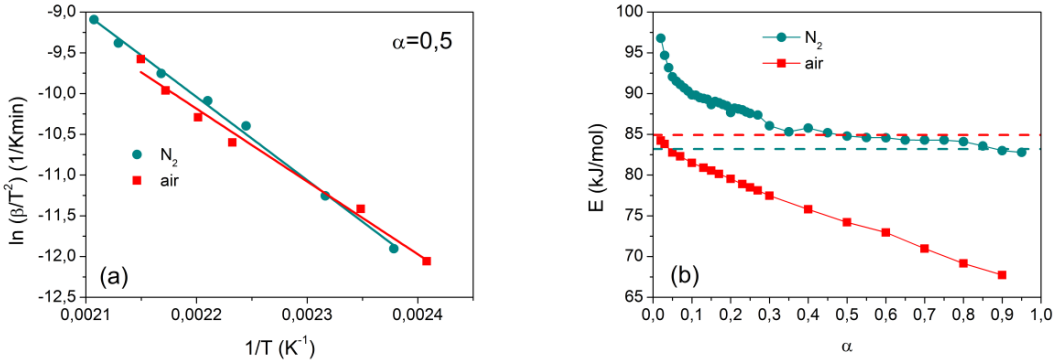

Fig. 4. *ln(β/T²)* vs. *1/T* plot (a) and *E* vs *α* plot (b) for TG measurements under N_2 and air performed for lauric acid.

The discrepancies in the results depending on the kinetic analysis method applied together with the variation of *E* with *α*, seem to indicate that a single-step reaction mechanism cannot be assumed for the thermal degradation of this acid. Actually, if we have a closer look to the dTG curves lauric acid under N_2 (Fig. 1(b)), we can see that they could be composed by two or more overlapped peaks. In our opinion, apart from evaporation, other additional reactions leading to volatile compounds may happen during the heating of lauric acid. Moreover, the fact that *E* values are lower in air than in N_2, seems to indicate that the presence of oxygen leads to different reactions that may accelerate the degradation process.

3.2. Deconvolution of dTG curves using Fraser-Suzuki functions

If a chemical reaction does not proceed in a single-step mechanism, a previous separation of the possible reaction processes should be carried out. A said above, this separation can be done by performing a deconvolution analysis of the dTG curves expressed in terms of conversion (*dα/dT*) by means of Fraser-Suzuki (*FS*) functions. If these functions are used in normalized form (i.e. the area under the curve is equal to 1), we can assume that each curve corresponds to an independent single-step reaction mechanism. The normalized *FS* function has the following mathematical expression:

$$\frac{d\alpha}{dT} = \left[\frac{2}{w}\exp\left(-\frac{s^2}{4\ln 2}\right)\left(\frac{ln2}{\pi}\right)^{1/2}\right]\exp\left\{-\frac{ln2}{s^2}\left[\ln(1+2s\frac{T-p}{w})\right]^2\right\} \qquad \text{(eq. 6)}$$

It contains three parameters: the peak-maximum position, *p*, the half-height width, *w*, and the asymmetry factor, *s*. Deconvolution can be done with two or more FS_n curves, each one with a certain contribution factor, C_n, to the final curve. This means that, in addition to the three parameters of each curve, the contribution factors must be included in the fitting process to the experimental *dα/dT* curves, which can be calculated as:

$$\left[\frac{d\alpha}{dT}\right]_\beta = \sum_1^n C_i * FS_i\,(p_i, w_i, s_i) \quad where \ \sum C_i = 1 \quad and \quad 0 < C_i < 1 \qquad \text{(eq. 7)}$$

If no restrictions are imposed to the parameters of (eq. 7), many combinations of FS_i and C_i may lead to good deconvolution results and it may happen that in the end it is not be possible to associate the obtained *FS* curves to any reaction mechanism. In order to overcome this issue, *dα/dT* curves were constructed from (eq. 2) for different reaction mechanisms (i.e., *f(α)* expressions) (Vyazovkin et al. 2011), various heating rates, *β*, and generic values of *E* and *A*. The resulting curves were fitted to the normalized Fraser-Suzuki function and the relationship between *FS* parameters (*p*, *w* and *s*) and the kinetic parameters (*f(α)*, *E*, *A* and *β*) was analyzed. The details of this study are out of the scope of this paper and will be reported in another work still under

preparation. The main conclusion of that study was that the asymmetry factor, *s*, depends only on the reaction mechanism, *f(α)*, remaining almost constant for any value of *E*, *A* and *β*. This means that specific values of *s* can be first checked for the FS_n functions used in the deconvolution in order to see which ones could lead to the best fitting. Moreover since we assume that each FS_n curve corresponds to a certain reaction mechanism, each curve should have not only the same *s* but also the same contribution factor C_n for all the heating velocities. This procedure requires the previous selection of a reaction mechanism through *f(α)* but it also reduces the freedom of the FS_n parameters and C_n making the deconvolution process more effective. The deconvolution of *dα/dT* curves was done with MATALB® software by using a self-made code.

The *dα/dT* curves of lauric acid measured under either N_2 or air, could be deconvolved by using only two *FS* curves. Different values of *s* were checked for each curve and it was concluded that the best fitting was achieved for s_1= -0.67 and s_2= between -0.35 and -0.38. The value of s_1 can be associated to a 1/2-order model (F05) while the values of s_2 can be associated to Avrami-Erofeev models (A2, A3 and A4) (Vyazovkin et al. 2011). In Table 2, the mathematical expressions of *f(α)* and *f'(α)* (to be used in Kissinger method) have been recorded together with the associated values of the *s* parameter in *FS* function.

Table 2. Mathematical expressions of *f(α)* and *f'(α)* with the associated values of s parameter of *FS* function.

Model ID	$f(\alpha)$	$f'(\alpha) = df(\alpha)/\alpha$	*s*
F05	$(1-\alpha)^{1/2}$	$-1/2(1-\alpha)^{-1/2}$	-0.67
An (2, 3, 4)	$n(1-\alpha)[-\ln(1-\alpha)]^{1/n}$	$-n[-\ln(1-\alpha)]^{(n-1)/n} + (n-1)[-\ln(1-\alpha)]^{-1/n2}$	[-0.35, -0.38]

The results of *dα/dT* curve deconvolution with two *FS* curves are displayed in Fig. 5 for lauric acid under N_2 at *β*= 1 ºC/min and 20 ºC/min (a) and under air at *β*= 2 ºC/min and 15 ºC/min (b). In N_2 atmosphere the contribution coefficients are 0.55 for FS_1 and 0.45 for FS_2 while, in air atmosphere, the contributions are 0.6 and 0.4 respectively. As we can see, the curves used in the deconvolution fit quite well the experimental *dα/dT* curves in the whole range of heating rates.

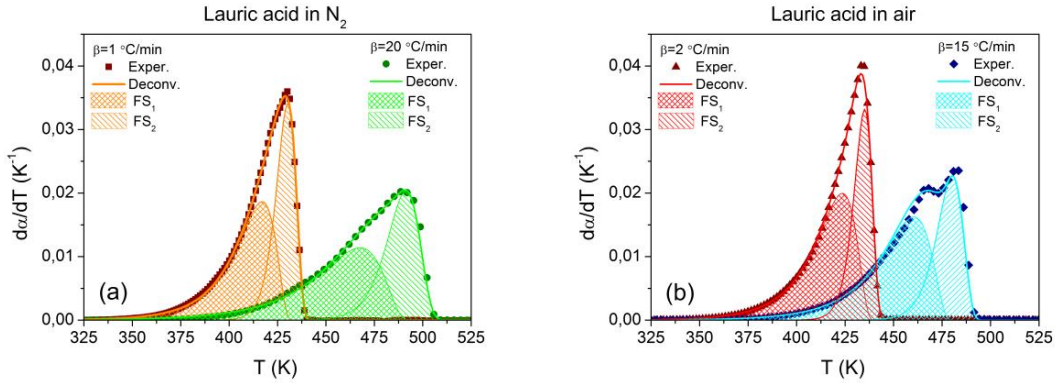

Fig. 5. Deconvolution results of *dα/dT* curves for lauric acid. Under N_2 at β= 1 ºC/min and 20 ºC/min (a) and under air at β= 2 ºC/min and 15 ºC/min (b).

3.3. Application of Kissinger method for calculating the Arrhenius parameters: *E* and log*A*

The *FS* curves resulting from the deconvolution process can be then treated as *dα/dT* curves associated to single-step reaction mechanisms. Moreover, since the deconvolution has been done by assuming some specific mechanisms, *f(α)*, the method of Kissinger (Kissinger, 1957) can be applied for obtaining the Arrhenius parameters. This method is derived from (eq. 1) under the condition of maximum reaction rate: $d^2\alpha/d\,t^2 = 0$ so that:

$$\frac{E\beta}{T_m^2} = -Af'(\alpha_m)e^{\left(\frac{-E}{RTm}\right)} \qquad \text{(eq. 8)}$$

Where $f'(\alpha_m) = \left[\frac{df(\alpha)}{d\alpha}\right]_{T_m}$ and the subscript *m* denotes the values related to the maximum.

After simple rearrangement, (eq. 8) is transformed into the Kissinger equation:

$$\ln\left(\frac{\beta}{T_m^2}\right) = \ln\left[-\frac{AR}{E}f'(\alpha_m)\right] - \frac{E}{RT_m} \qquad \text{(eq. 9)}$$

If the mathematical expression of $f(\alpha)$ is known, $f'(\alpha_m)$ can be calculated (see Table 2) and the frequency factor, A, obtained from the intercept of the liner plot since E is given by the slope. It must be pointed out that although it seems that the left hand terms of (eq. 5) and (eq. 9) are the same, they are not because they are derived from different assumptions. Actually the Kissinger method yields a reliable estimation of E only if α_m does not vary significantly with β. This happens for many reaction models (Braun and Burnham, 1987; Cheng et al., 1993) but not for all models. Hence the independence of α_m with β has to be checked before applying this method. In our case, α_m remained constant for all the values of β for both sets of FS curves (see Table 3), so that we could apply the Kissinger method for obtaining the Arrhenius parameters of each single-step reaction mechanism.

The Kissinger plots of both FS_1 and FS_2 sets of curves for lauric acid under N_2 and air are displayed Fig. 6 (a) and (b) respectively. From the slope of the linear plots, E was calculated for each single-step reaction mechanism. For calculating the pre-exponential factor, A, from the intercept of the linear fit, the $f'(\alpha)$ associated to the expected reaction mechanism must be taken. For the case of FS_2 curves, the $f'(\alpha)$ associated to three Avrami-Erofeev mechanisms were checked and the corresponding A values were calculated. In order to determine which Avrami-Erofeev mechanism was the most appropriate, $d\alpha/dT$ curves were simulated for each of them using (eq. 2) and the Arrhenius parameters obtained with Kissinger method. These curves were compared with the FS_2 curves so that the most appropriate mechanism could be established. In the end the Avrami-Erofeev mechanism that better fitter FS_2 set of curves was the A3 for the case of lauric acid under N_2 and the A4 for the case of lauric acid under air (see Table 3).

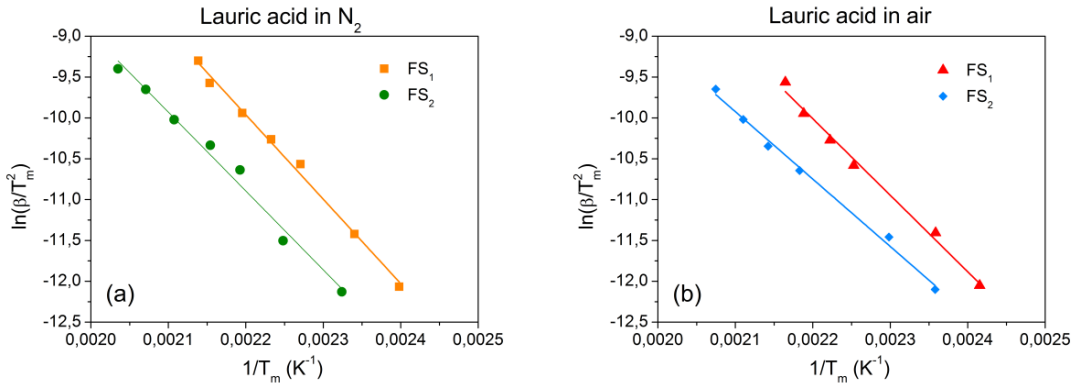

Fig. 6. Kissinger plots of the FS curves obtained in the deconvolution of experimental dα/dT curves for lauric acid under N_2 (a) and air (b) atmospheres.

Once the kind of Avrami-Erofeev model was identified, both deconvolutions and Kissinger plots were further refined. The final values of the Arrhenius parameters E and $logA$ (min^{-1}) are the ones recorded in Table 3. In terms of activation energy, the values obtained with the Kissinger method are in the range of the ones displayed in the E vs. α plots of Fig. 4 (b), being lower for lauric acid under air than for lauric acid under N_2.

Table 3. Contribution coefficient and Arrhenius parameters obtained by Kissinger method for the two reaction mechanisms proposed for the thermal degradation of lauric acid under N_2 and under air.

Atmosphere	FS_n curve	C_n	Model ID	E (kJ/mol)	α_m	$logA$ (min^{-1})
N_2	FS_1	0.55	F05	85.9±1	0.715	9.59
N_2	FS_2	0.45	A3	80.2±1	0.620	8.51
air	FS_1	0.6	F05	77.8 ±1	0.715	8.60
air	FS_2	0.4	A4	68.6±1	0.620	7.15

In principle, the F05 mechanisms identified in the thermal degradation of lauric acid for FS_1 could be associated to the evaporation process, since $d\alpha/dT$ curves calculated with (eq. 2) for both zero-order and 1/2-order mechanism with the same Arrhenius parameters are quite coincident in the temperature range below the maximum rate. As for the activation energies recorded in Table 3 associated to the F05 mechanism, they are both different from the values obtained from the plot of (eq. 4). However, if we take into account that 10% error in the activation energy is quite reasonable in any kinetic analysis (Vyazovkin et al. 2011), we can assume that FS_1 curves can be associated to the evaporation of lauric acid which can be represented by a 1/2-order mechanism with E=83±8 kJ/mol. In order to support this assumption, $d\alpha/dT$ curves were constructed by using (eq. 2) for 1/2-order mechanism, $f(\alpha) = (1-\alpha)^{1/2}$, with the Arrhenius parameters recorded in Table 3 for both N_2 and air atmospheres at various heating rates and then fitted to single FS functions. The variation of the parameter p (i. e. peak-maximum position) with the heating rate, β, for both atmospheres is displayed in Fig. 7. The values of p parameter corresponding to the FS_1 curves resulting from the deconvolution of the experimental $d\alpha/dT$ curves have been included as well. As we can observe, the values of p are not very different for the F05 curves simulated with the Arrhenius parameters either for the case of N_2 or for the case of air. Moreover the p values of the FS_1 curves resulting from the deconvolution process are also very close the values obtained for the simulated F05 curves.

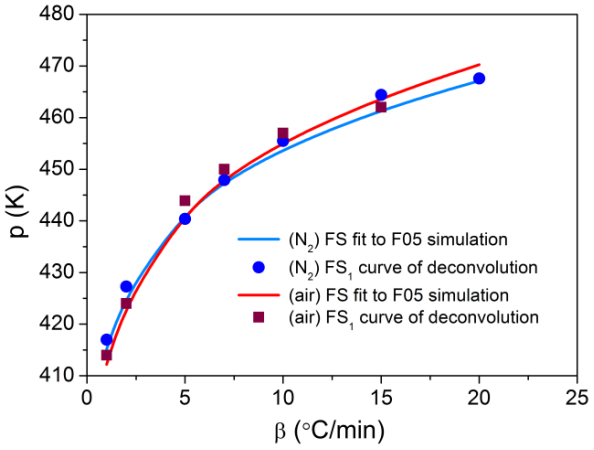

Fig. 7. Plot of p vs. β for FS curves resulting from the fitting of F05 curves and the deconvolution of experimental $d\alpha/dT$ curves of lauric acid under N_2 and air.

For the case of FS_2 curves, Avrami-Erofeev mechanism (A3) is associated to three dimensional nucleation processes and the A4 to a four dimensional nucleation. Since we do not have information about the reaction products we cannot propose possible reactions processes that can be related to any Avrami-Erofeev mechanism. In order to elucidate the reactions that my occur during thermal degradation of lauric acid, TG measurements with the analysis of the evolved gases would be required, especially in the case of the measurements under air since this is the most conventional atmosphere in which PCM operate when they are implemented in latent heat storage modules.

3.3. Construction of α vs. T curves

Once the kinetic triplet is determined, (eq. 3) can be used for constructing the α vs. T curves at different heating velocities and comparing them with the experimental TG curves. In Fig. 8 some of these curves are displayed for the case of lauric acid under N_2 (a) (β=1, 5, 20 ºC/min) and under air (b) (β=2, 5, 15 ºC/min). In both cases we can see that the calculated curves fit very well the experimental curves for all the heating velocities.

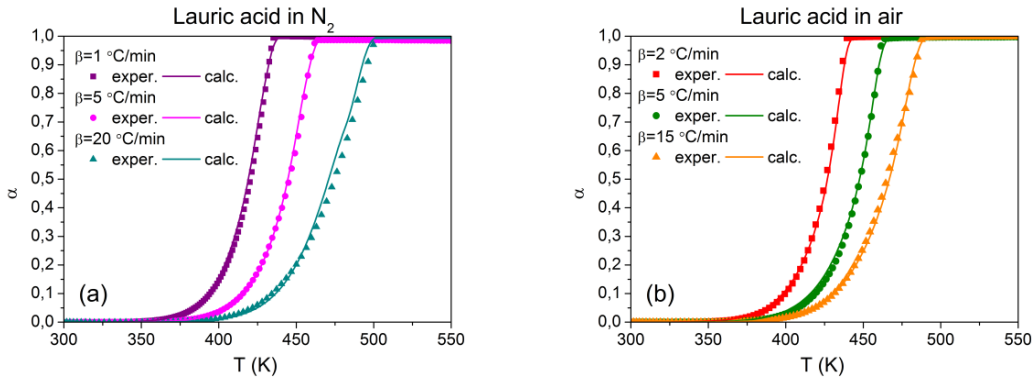

Fig. 8. Calculated α vs. T curves for lauric acid under N_2 (a) and air (b) at various heating velocities, β. Comparison with the experimental TG curves expressed in terms of α.

3.4. Construction of the isothermal degradation curves

Isothermal degradation or ageing time curves can be constructed by rearranging (eq. 1) and integrating at constant temperature:

$$\int_0^t dt = \frac{1}{Ae^{\left(\frac{-E}{RT}\right)}} \int_0^\alpha \frac{d\alpha}{f(\alpha)} \qquad \text{(eq. 10)}$$

$$t = \frac{g(\alpha)}{Ae^{\left(\frac{-E}{RT}\right)}} \qquad \text{(eq. 11)}$$

Hence from the expression of the *g(α)* function we can obtain the relationship between the ageing time, *t*, and the corresponding conversion, *α*. Here, *g(α)* is a combination of two independent mechanisms, each of them with their corresponding Arrhenius parameters and contribution to the whole conversion. Therefore the curve of (eq. 11) must also contain the contribution of the independent mechanisms. The *g(α)* expressions associated to the mechanisms proposed for the thermal degradation of lauric acid are displayed in Table 4.

Table 4. Mathematical expressions of *g(α)* for the reaction mechanisms proposed for lauric acid thermal degradation.

Model ID	$g(\alpha)$
F05	$\frac{1-(1-\alpha)^{0.5}}{0.5}$
A3	$[-\ln(1-\alpha)]^{1/3}$
A4	$[-\ln(1-\alpha)]^{1/4}$

The isothermal degradation curves calculated for lauric acid under N_2 and under air at both 50ºC (T_m+5 ºC) and 55 ºC (T_m+10 ºC) are displayed in Fig. 9. As we can see, lauric acid degrades faster under air than under N_2, which is not surprising since the activation energies for this acid in air are lower. However, according to these curves, even if lauric acid is kept under N_2 at 50 ºC (i.e., 5 ºC above the melting temperature), its mass should have disappeared from the container in less than one month. In order to check these predictions, some preliminary isothermal tests with samples in the range of grams have been performed in an oven at 50ºC under air and no variation of sample mass has been observed for several weeks. Actually since evaporation (and gas emission) is a surface phenomenon, it is reasonable to assume that the rate of loss of molecules from a given volume is not only proportional to the sample mass but also to the molecules exposed on the surface (Penner, 1952). Hence, if sample mass is very low and vapor molecules are removed by a carrier, which is the case of TG measurements that are always performed under a gas flow, evaporation and gas emission processes will be faster and so will be the mass loss. This indicates that the kinetic analysis of TG measurements must be complemented with experiments inside an oven under isothermal conditions with samples of larger mass. This should allow extrapolating the degradation processes to the real operation conditions and hence obtaining more reliable isothermal degradation curves.

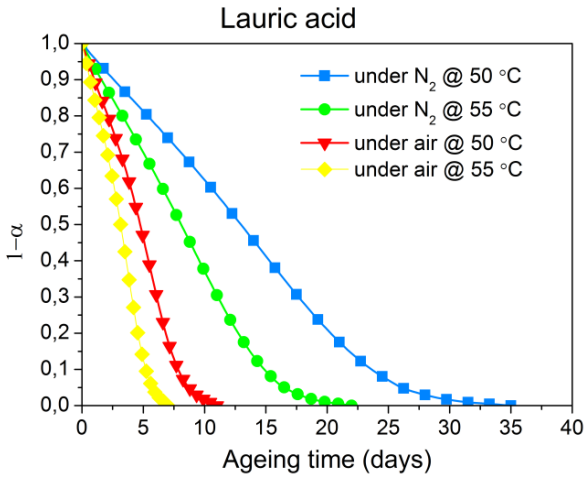

Fig. 9. Isothermal degradation curves for lauric acid under N_2 and under air at both 50ºC (T_m+5 ºC) and 55 ºC (T_m+10 ºC).

4. Conclusions and future actions

In this work, the kinetic analysis of TG measurements under both N_2 and air atmospheres has been carried out for lauric acid, a straight-chain fatty acid normally used as a PCM for latent heat storage in low temperature applications. In a first approach, Arrhenius parameters were calculated assuming a zero-order evaporation process with the resulting activation energy very close to the evaporation enthalpy. However the experimental *dα/dT* curves could not be simulated by only considering the evaporation of lauric acid. By using a model-free isoconversional method we found that the activation energy varied significantly with the conversion so that a multi-step processes should be assumed for lauric acid thermal degradation. From a deconvolution analysis of *dα/dT* curves two single-step reaction mechanisms could be proposed. One of the mechanisms was associated to the evaporation since its activation energy was within 10% error range of the evaporation enthalpy. The other mechanism could be related to the evolution of volatile compounds but the corresponding reaction paths are still undetermined. Since the activation energy value of this second mechanism was lower when lauric acid was heated up in air, it is very likely that O_2 is involved in the process. According to the isothermal degradation curves, it is expected that lauric acid totally disappears after 30 days when kept under N_2 at 5 ºC above its melting temperature. However, the long-term non-stability of lauric acid cannot be confirmed yet since some preliminary isothermal experiments inside an oven have shown that it does not behave as predicted by these curves. As part of future actions, we can say that the kinetic analysis would be improved if evolved gases were analyzed since this would help identifying which reactions are taking place apart from evaporation. Moreover chemical changes without gas emission could happen as well. Keeping in mind that assessing the long-term stability is our goal, isothermal experiments in oven with larger amounts of sample are necessary for obtaining isothermal degradation curves that are more reliable and representative of the degradation processes occurring under real operation conditions. The same kind of kinetic analysis should be carried out for the rest of fatty acids we have considered as PCM for latent heat storage in low-temperature applications.

5. Acknowledgments

This work has been supported by Comunidad de Madrid and European Structural Funds through ACES2030 Project (S2018/EM-4319) and by European Union's Horizon H2020 Research and Innovation Programme through SFERA III Project (GA Nº 823802).

6. References

Arias, S., Prieto, M. M., Ramajo, R., Espina, A., García, J. R., 2009. Model free kinetics applied to the evaporation of caprylic acid. J. Therm. Anal. Calorim. 98, 457-462.

Akahira, T., Sunose, T., 1971. Method of determining activation deterioration constant of electrical insulating materials. Res. Report Chiba Inst. Technol. (Sci. Technol.) 16, 22–31.

Bayón, R., Rojas, E., 2019. Development of a new methodology for validating thermal storage media: Application to phase change materials. Int. J. Energy Res. 43, 6521-6541.

Braun, R. L., Burnham, A. K., 1987. Analysis of chemical reaction kinetics using a distribution of activation energies and simpler models. Energy Fuels 1, 153-161.

Cheng, D., Gao, X., Dollimore, D., 1993. A generalized from of the Kissinger equation. Thermochim. Acta 215, 109-117.

Cheng, Z., Wu, W., Ji, P., Zhou, X., Liu, R., Cai, J., 2015. Applicatility of Fraser-Suzuki function in kinetic analysis of DAEM processes and lingnocellulosic biomass pyrolysis process. J. Therm. Anal. .Calorim. 119, 1429-1438.

Coats, W., Redfern, J. P., 1964. Kinetic parameters from thermogravimetric data. Nature 201, 68.

Doyle, C. C., 1961. Kinetic analysis of thermogravimetric data. J. Appl. Polym. Sci. 5 (15), 285-292.

Fraser, R. D. B., Suzuki, E., 1969. Resolution of overlapping bands: functions for simulating band shapes. Anal. Chem. 41(1), 37-39.

Güneş, M., Güneş, S., 1999. The influences of various parameters on the numerical solution of nonisothermal DAEM equation. Thermochim. Acta 336, 73-96.

Kahwaji, S., Johnson, M. B., Kheirabadi, A. C., Groulx, D., White, M. A., 2017. Fatty acids and related phase change materials for reliable thermal energy storage at moderate temperatures. Sol. Energy Mater. Sol. Cells. 167, 109-120.

Kissinger, H. E,, 1957. Reaction kinetics in differential thermal analyisis. Anal. Chem. 29, 1702-1706.

Miura, K., Maki, T., 1998. A simple method for estimating f(E) and k0(E) in the distributed activation energy model. Energy Fuels 12(5), 864-869.

Órfão, J., 2007 Review and evaluation of the approximations to the temperature integral. AICHE J. 31 (11), 2905-2915.

Penner, S. S., 1952. On the kinetics of evaporation. J. Phys. Chem. 56(4), 475-479

Perejón, A., Sáncez-Jiménez, P. E., Criado J. M., Pérz-Maqueda, L. A., 2011. Kinetica of complex solid-state reactions. A new deconvolution procedure. J. Phys. Chem. B 115, 1780-1791.

Rusch, P. F., Lelieur, J. P., 1973. Analytical moments of skewed gaussian distribution functions. Anal. Chem. 45(8), 1541-1543.

Shen, L., Alexander, K. S., 1999. A thermal analysis of long chain fatty acids. Thermochim. Acta 340-341, 271-278.

Stankovic, B., Jovanovic, J., Adnadjevic, B., 2018. Application of the Suzuki–Fraser function in modelling the non-isothermal dehydroxylation kinetics of fullerol. React. Kinet. Mech. Cat. 123 (2), 421-438.

Vyazovkin, S., Burnham, A. K.,Criado, J. M., Pérez-Maqueda, L. A., Popescu, C., Sbirrazzouli, N., 2011. ICTAC Kinetics Committee recommendations for performing kinetic computations on thermal analysis data. Thermochim. Acta 520, 1-19.

Vyazovkin, S., Burnham, A. K., Favergeon, L., Koga, N., Moukhina, E., Pérez-Maqueda, L. A., Sbirrazzouli, N., 2020. ICTAC Kinetics Committee recommendations for analysis of multi-step kinetics. Thermochim. Acta 689, 178597